

## Orientation distribution of cylindrical particles suspended in a turbulent pipe flow

Ling-Xin Zhang, Jian-Zhong Lin, and T. L. Chan

Citation: *Phys. Fluids* **17**, 093105 (2005); doi: 10.1063/1.2046713

View online: <http://dx.doi.org/10.1063/1.2046713>

View Table of Contents: <http://pof.aip.org/resource/1/PHFLE6/v17/i9>

Published by the [American Institute of Physics](#).

---

### Related Articles

Clouds of particles in a periodic shear flow

*Phys. Fluids* **24**, 021703 (2012)

The dynamics of a vesicle in a wall-bound shear flow

*Phys. Fluids* **23**, 121901 (2011)

A study of thermal counterflow using particle tracking velocimetry

*Phys. Fluids* **23**, 107102 (2011)

Particle accumulation on periodic orbits by repeated free surface collisions

*Phys. Fluids* **23**, 072106 (2011)

Drag force of a particle moving axisymmetrically in open or closed cavities

*J. Chem. Phys.* **135**, 014904 (2011)

---

### Additional information on Phys. Fluids

Journal Homepage: <http://pof.aip.org/>

Journal Information: [http://pof.aip.org/about/about\\_the\\_journal](http://pof.aip.org/about/about_the_journal)

Top downloads: [http://pof.aip.org/features/most\\_downloaded](http://pof.aip.org/features/most_downloaded)

Information for Authors: <http://pof.aip.org/authors>

### ADVERTISEMENT



**Running in Circles Looking  
for the Best Science Job?**

Search hundreds of exciting  
new jobs each month!

<http://careers.physicstoday.org/jobs>

physicstodayJOBS



## Orientation distribution of cylindrical particles suspended in a turbulent pipe flow

Ling-Xin Zhang and Jian-Zhong Lin<sup>a)</sup>

*Department of Mechanics, State Key Laboratory of Fluid Power Transmission and Control, Zhejiang University, Hangzhou, 310027, China*

T. L. Chan

*Research Centre for Combustion and Pollution Control, Department of Mechanical Engineering, The Hong Kong Polytechnic University, Hung Hom, Kowloon, Hong Kong*

(Received 10 January 2005; accepted 20 July 2005; published online 21 September 2005)

A model of turbulent cylindrical particle suspensions is proposed to predict the orientation distribution of particles. The fluctuating equation for the orientation distribution function (ODF) of cylindrical particles is theoretically solved using the method of characteristics. The orientation-correlated terms in the mean equation for the ODF due to the random motion of cylindrical particles are related to the correlations of the mean ODF and the fluid velocity gradient. Thus, the evolution of the mean ODF is described by a modified convection-dispersion equation. The model and modified equation are used to calculate the ODF in a pipe flow numerically. The results compare qualitatively with the experimental data and show that the turbulent dispersion makes cylindrical particles have a broad orientation distribution, while the velocity gradient plays an opposite role. The increase of the particle aspect ratio leads to a less aligned distribution in the vicinity of the axis and a narrower orientation distribution at positions far from the axis.

© 2005 American Institute of Physics. [DOI: [10.1063/1.2046713](https://doi.org/10.1063/1.2046713)]

### I. INTRODUCTION

It has been known that the physical properties of solid particle suspensions mostly depend on the particle spatial distribution. For nonspherical particles such as cylindrical particles, the particle orientation becomes another important parameter. Understanding the microstructure of cylindrical particle suspensions during flows is currently of great interest in many areas, including polymer suspensions, fiber composite process, and pulp and papermaking industry. Many theoretical and experimental works were performed in this field, focusing on the fundamental study in some simple flows, such as simple shear flow and irrotational extensional flow. The present work is to provide a new model for prediction of orientation distribution of cylindrical particles suspended in turbulent shear flows.

The factors affecting the particle orientation include velocity gradient, external forces, or torques, and randomizing factors such as hydrodynamic interactions among particles,<sup>1,2</sup> rotational Brownian motion,<sup>3,4</sup> or local turbulent motion. For dilute suspensions and in the absence of external forces and Brownian motion, the mean velocity gradient and the randomizing effect of turbulence are the dominant factors.

For laminar flows the orientation of nonspherical particles depends on the fluid velocity gradient and the parameter of particle shapes. Several investigators<sup>5-7</sup> have studied the motion of nonspherical particles and the particle orientation distribution. On the basis of the Fokker-Planck equation a theoretical analysis can be carried out. Note that for simple

shear flows the orientation distribution of cylindrical particles is independent of the shear rate, and the total time reaching the steady distribution state increases with the decrease of shear rate.

For turbulent flows the randomizing effect of turbulent fluids becomes an important additional factor. There are two methods to model turbulent particle suspensions, the Lagrangian approach and the Eulerian approach. For the former the concentration and orientation distributions of particles are the statistical results of their trajectories, which are obtained by solving the translation and rotation equations of a single particle through a known flow field. This approach has been used to estimate the distribution of cylindrical particles suspended in turbulent flows.<sup>8-10</sup> In the Eulerian approach, the probability distribution function of particle orientation and position is calculated using a Fokker-Planck equation or convection-dispersion equation. This approach has several advantages for modeling the turbulent particle suspensions, for example, it is computationally more efficient and has the potential to account for the particle-particle and the particle-fluid interactions. On the basis of the Eulerian approach, the orientation distribution function (ODF) of small fibers in turbulent flow has been theoretically calculated by Krushkal and Gallily.<sup>11</sup> A key parameter in such flows was the rotational Peclet number, which is the ratio of a typical velocity gradient to the rotational dispersion coefficient. Recently, Olson and Kerekes<sup>12</sup> obtained fiber translational and rotational dispersion coefficients with the assumption that the relative velocity of particle and fluid can be neglected. They related the dispersion coefficients to the Lagrangian particle velocity correlation. This model, however, is limited to homogeneous isotropic turbulent flows.

<sup>a)</sup> Author to whom correspondence should be addressed. Electronic mail: [jlzlin@sfp.zju.edu.cn](mailto:jlzlin@sfp.zju.edu.cn)

For suspensions in the shear flows Feng and Leal<sup>13</sup> simulated liquid-crystal polymer (LCP) channel flows in order to examine how contractions and expansions in a channel affect LCP orientation and to explore the possibility of using the channel geometry as a means of manipulating LCP order. Lyon *et al.*<sup>14</sup> studied experimentally the evolution of the particle microstructure for noncolloidal particles that are suspended in a viscoelastic medium and subjected to steady and oscillatory shear flows, and they presented new results of the particle microstructure for a dilute bidisperse system. Sgalari *et al.*<sup>15</sup> investigated the textural evolution of liquid-crystal polymer systems under planar shear at high shear rates, and they identified the mechanisms at play and the relative roles of the various forces in determining the evolution of texture at moderate shear rates.

The effect of turbulent dispersion, velocity gradient, and particle aspect ratio on the orientation distribution of cylindrical particles in the turbulent suspension of shear flows appears to be an unexplored topic. Therefore, the aims of the present work are to develop a model of turbulent cylindrical particle suspensions valid for shear flows and theoretically solve the fluctuating equation for the ODF of cylindrical particles. Finally, the model is applied to a pipe flow and some of the numerical results of the orientation distribution are compared with the measured data given by Bernstein and Shapiro.<sup>16</sup>

## II. THEORY ON ORIENTATIONAL DISPERSION

In this section, an analysis is carried out on the governing equation for the ODF in the planar shear flow. For laminar flows, the analytic results of the orientation distribution of cylindrical particles in a wide range of aspect ratios are obtained. For turbulent flows, the fluctuating equation for the ODF is solved and the orientation-correlated terms are related to the gradients of the mean ODF. Finally, an expression for the turbulent orientational diffusivity, which accounts for the flux opposite to the gradient of the particle orientation distribution, is derived.

### A. Definition

Theoretical models for predicting the rheological behavior of nonspherical particle suspensions explicitly account for the particle orientation distribution. Using the slender-body theory, Batchelor<sup>17</sup> gave the constructive equation for the stress in the suspensions of slender particles:

$$\boldsymbol{\sigma} = 2\mu\mathbf{s} + \mu_p \left( \langle \mathbf{p}\mathbf{p}\mathbf{p}\mathbf{p} \rangle - \frac{1}{3} \mathbf{I} \langle \mathbf{p}\mathbf{p} \rangle \right) : \mathbf{s}, \quad (1)$$

where  $\boldsymbol{\sigma}$  the stress tensor,  $\mathbf{p}$  is a unit vector parallel to the particle axis,  $\mathbf{I}$  is the unit tensor,  $\mathbf{s} = (\nabla\mathbf{u} + \nabla\mathbf{u}^T)/2$  is the rate of the strain tensor,  $\mu$  is the viscosity of the suspending fluid,  $\mu_p$  is the additional viscosity due to the presence of particles, and the angle brackets denote an average over the orientation distribution:

$$\langle \mathbf{p}\mathbf{p} \rangle = \oint \mathbf{p}\mathbf{p}\psi(\mathbf{p})d\mathbf{p}, \quad (2)$$

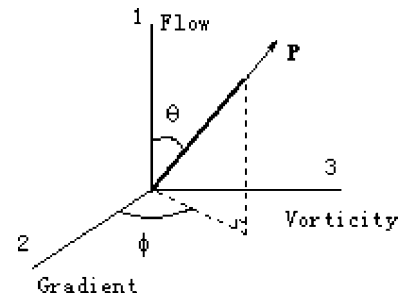


FIG. 1. A cylindrical particle in the spherical coordinate system.

$$\langle \mathbf{p}\mathbf{p}\mathbf{p}\mathbf{p} \rangle = \oint \mathbf{p}\mathbf{p}\mathbf{p}\mathbf{p}\psi(\mathbf{p})d\mathbf{p}. \quad (3)$$

Here  $\psi$  is the ODF, which characterizes the probability density of realization of each specific orientation. This function satisfies the normalization condition:

$$\oint \psi(\mathbf{p})d\mathbf{p} = 1. \quad (4)$$

A suspension of  $n$  rigid, cylindrical particles per unit volume is considered; each particle has length  $L$  and diameter  $D$ , and  $a=L/D$  is the particle aspect ratio. It is assumed that there are no concentration gradients so that  $n$  is a constant. Particle concentration limits in the range of  $nL^3 \ll 1$ , which means that the suspension is dilute.

The function of particle inertia has been discussed by Bernstein and Shapiro.<sup>16</sup> In their work, the particle inertia is neglected, so the center of mass translates affinely with the bulk flow. A torque balance about the center of mass leads to the equation of motion for the orientation vector  $\mathbf{p}$ .<sup>18</sup>

$$\dot{\mathbf{p}} = \mathbf{k} \cdot \mathbf{p} - \mathbf{k} : \mathbf{p}\mathbf{p}\mathbf{p}, \quad (5)$$

where  $\dot{\mathbf{p}}$  is the time derivative of  $\mathbf{p}$ , i.e.,  $D\mathbf{p}/Dt$ , the unit vector  $\mathbf{p}$  has the following form in the spherical coordinate system (see Fig. 1):

$$\begin{aligned} p_1 &= \cos \theta, \\ p_2 &= \sin \theta \cos \phi, \\ p_3 &= \sin \theta \sin \phi, \end{aligned} \quad (6)$$

and  $\mathbf{k} = \nabla\mathbf{u}^T$  is the fluid velocity gradient tensor. The above equation of motion shows that the orientation vector  $\mathbf{p}$  changes as though it was an element of the fluid,  $(\mathbf{k} \cdot \mathbf{p})$ , except that it cannot stretch, so the stretching part of the motion,  $(\mathbf{k} : \mathbf{p}\mathbf{p}\mathbf{p})$ , is subtracted off.

Equation (5) is only valid for the particles with infinite aspect ratio. Jeffery<sup>5</sup> first determined the motion of a single slender particle in an unbounded linear flow field for a Newtonian medium. He showed that a particle rotates in one of a family of closed orbits around the vorticity axis. The particle spends a relatively long time orientating within an angle  $O(1/a)$  near the flow-vorticity plane, then flips rapidly until it becomes nearly aligned again. Jeffery's results had been used by several authors<sup>7,11,19</sup> to study the orientation distri-

bution of cylindrical particles with finite aspect ratios, and the time derivative of the vector  $\mathbf{p}$  is given by

$$\dot{\mathbf{p}} = -\mathbf{w} \cdot \mathbf{p} + \lambda \mathbf{s} \cdot \mathbf{p} - \lambda \mathbf{s} : \mathbf{p} \mathbf{p} \mathbf{p}, \quad (7a)$$

where  $\dot{\mathbf{p}}$  refers to  $D\mathbf{p}/Dt$ ,  $\lambda$  is a parameter of particle aspect ratio and equals to  $(a^2-1)/(a^2+1)$ , and  $\mathbf{w} = (\nabla \mathbf{u} - \nabla \mathbf{u}^T)/2$  is the vorticity tensor. Considering  $\mathbf{w} : \mathbf{p} \mathbf{p} = 0$ , Eq. (7a) can be changed to the form similar to Eq. (5):

$$\dot{\mathbf{p}} = (\lambda \mathbf{s} - \mathbf{w}) \cdot \mathbf{p} - (\lambda \mathbf{s} - \mathbf{w}) : \mathbf{p} \mathbf{p} \mathbf{p}. \quad (7b)$$

For the particle with infinite aspect ratio ( $\lambda=1$ ), Eq. (7b) is same as Eq. (5).

The governing equation for the ODF depends on the conservation of cylindrical particles in the orientation space. The transient equation for the ODF is given by

$$\frac{\partial \psi}{\partial t} + \frac{\partial(\psi \dot{\mathbf{p}})}{\partial \mathbf{p}} = 0. \quad (8)$$

It shows that the rotation of particle makes the orientation distribution change and the ODF of particles is determined by the fluid velocity gradient tensor.

## B. Analytic solution in laminar shear flow

In the spherical coordinate system  $(R, \theta, \phi)$  as shown in Fig. 1, the unit vectors in the three directions are

$$\delta_R = c_\theta \mathbf{e}_1 + s_\theta c_\phi \mathbf{e}_2 + s_\theta s_\phi \mathbf{e}_3, \quad (9)$$

$$\delta_\theta = -s_\theta \mathbf{e}_1 + c_\theta c_\phi \mathbf{e}_2 + c_\theta s_\phi \mathbf{e}_3, \quad (10)$$

$$\delta_\phi = -s_\phi \mathbf{e}_2 + c_\phi \mathbf{e}_3, \quad (11)$$

where  $s_\theta = \sin \theta$ ,  $c_\theta = \cos \theta$ ,  $s_\phi = \sin \phi$ , and  $c_\phi = \cos \phi$ . In this system, the steady-state equation for the ODF has the following form:

$$\frac{1}{s_\theta} \frac{\partial(s_\theta \dot{\theta} \psi)}{\partial \theta} + \frac{\partial(\dot{\phi} \psi)}{\partial \phi} = 0 \quad (12)$$

or

$$\dot{\theta} \frac{\partial \psi}{\partial \theta} + \dot{\phi} \frac{\partial \psi}{\partial \phi} + \chi \psi = 0, \quad (13)$$

where  $\dot{\theta}$  and  $\dot{\phi}$  are the time derivatives of  $\theta$  and  $\phi$ , respectively, i.e., the angular velocities, and  $\chi$  characterizes the compressibility in the orientation space:

$$\dot{\theta} = (\lambda \mathbf{s} - \mathbf{w}) : \delta_R \delta_\theta, \quad (14)$$

$$\dot{\phi} = \frac{1}{s_\theta} \cdot (\lambda \mathbf{s} - \mathbf{w}) : \delta_R \delta_\phi, \quad (15)$$

$$\chi = (\lambda \mathbf{s} - \mathbf{w}) : \delta_R \delta_R. \quad (16)$$

For simple shear flows, the velocity gradient tensor has only one nonzero component,  $k_{12}$ , so we let  $k_{12} = \dot{\gamma}$ . Then the above equations can be given by:

$$\dot{\theta} = \frac{1}{2} (\lambda c_{2\theta} - 1) c_\phi \dot{\gamma}, \quad (17)$$

$$\dot{\phi} = \frac{1 - \lambda c_\theta}{2} \frac{c_\theta}{s_\theta} s_\phi \dot{\gamma}, \quad (18)$$

$$\chi = -3\lambda s_\theta c_\theta c_\phi \dot{\gamma}. \quad (19)$$

For the particles with large aspect ratio ( $\lambda \rightarrow 1$ ),  $\dot{\phi}$  is very small according to Eq. (18) and can be neglected. Applying this result, we can now solve Eq. (13) with the boundary condition:

$$\psi(\theta = \pi/2) = f_0(\text{const}). \quad (20)$$

The solution of Eq. (13) is

$$\psi = f_1 (1 - \lambda c_{2\theta})^{-3/2}, \quad (21)$$

where  $f_1$  is a constant determined by the normalization condition (4). Note that the orientation angle  $\phi$  is dependent on the initial conditions. Here,  $\phi$  has a uniform distribution initially.

For the particles with infinite aspect ratio ( $\lambda=1$ ), we have  $\psi \sim 1/\sin^3 \theta$  from Eq. (21), i.e.,  $\psi \rightarrow \infty$  at  $\theta=0$ , which indicates that all particles are aligned with the flow direction. A similar expression,  $\psi \sim f_1(\phi)/\sin^3 \theta$ , has been used by Rahnema *et al.*<sup>2</sup> to estimate the hydrodynamic interactions between particles. While for the particles with finite aspect ratios,  $\psi$  has a finite value at  $\theta=0$ , which means that the majority of the particles are nearly aligned with the flow direction, and only a small  $O(1/a)$  fraction of particles is flipping at any given time.

## C. Orientational dispersion in turbulent shear flow

### 1. Mean and fluctuating equations

For turbulent suspensions, the particles undergo mean motion due to the mean fluid velocity and random motion due to the fluctuating component of the fluid velocity. To estimate the randomizing effect of turbulence on the behavior of the cylindrical particles, the ODF is divided into two parts:

$$\psi = \bar{\psi} + \psi', \quad (22)$$

where  $\bar{\psi}$  is the ensemble average of  $\psi$ , and  $\psi'$  is the fluctuating part of  $\psi$ . Averaging Eq. (12), we obtain the equation for the mean ODF:

$$\frac{1}{s_\theta} \frac{\partial(s_\theta \bar{\theta} \bar{\psi})}{\partial \theta} + \frac{\partial(\bar{\phi} \bar{\psi})}{\partial \phi} = \bar{P}, \quad (23)$$

then subtracting the above equation from Eq. (12) we get the equation for  $\psi'$ :

$$\frac{1}{s_\theta} \frac{\partial(s_\theta \bar{\theta} \psi')}{\partial \theta} + \frac{\partial(\bar{\phi} \psi')}{\partial \phi} = Q, \quad (24)$$

where  $\bar{\theta}$  and  $\bar{\phi}$  are the components of mean angular velocities,  $\bar{P}$  and  $Q$  have the following forms:

$$\bar{P} = -\frac{1}{s_\theta} \frac{\partial(s_\theta \bar{\theta}' \bar{\psi}')}{\partial \theta} - \frac{\partial(\bar{\phi}' \bar{\psi}')}{\partial \phi}, \quad (25)$$

$$Q = -\frac{1}{s_\theta} \frac{\partial(s_\theta \dot{\theta}' \bar{\psi})}{\partial \theta} - \frac{\partial(\dot{\phi}' \bar{\psi})}{\partial \phi}, \quad (26)$$

and  $\dot{\theta}'$  and  $\dot{\phi}'$  are the fluctuating angular velocities and are given by

$$\dot{\theta}' = (\lambda s' - w') : \delta_R \delta_\theta, \quad (27)$$

$$\dot{\phi}' = \frac{1}{s_\theta} \cdot (\lambda s' - w') : \delta_R \delta_\phi. \quad (28)$$

The term  $\bar{P}$  on the right side of Eq. (23) accounts for the effect of turbulence on the ODF of cylindrical particles. Equation (23) is the key equation to describe the mean motion of the cylindrical particles suspended in turbulent flows. However, the evolution of the mean ODF depends on the coupling between the mean motion and the fluctuating motion. The angular velocity-ODF correlated terms in expression (25) are related to  $\psi'$ .

## 2. Solution of $\psi'$

Using the method of characteristics, Eq. (24) for  $\psi'$  can be changed to three differential equations:

$$\frac{d\theta}{d\tau} = \bar{\theta}, \quad (29)$$

$$\frac{d\phi}{d\tau} = \bar{\phi}, \quad (30)$$

$$\frac{d\psi'}{d\tau} + \bar{\chi} \psi' = Q, \quad (31)$$

where  $\bar{\theta}$ ,  $\bar{\phi}$ , and  $\bar{\chi}$  have the same forms as Eqs. (17)–(19) if we let  $\bar{k}_{12} = \dot{\gamma} \neq 0$  for turbulent shear flows.

For laminar shear flows, the steady-state ODF is very small at  $\theta = \pi/2$  (plane 2-3 as shown in Fig. 1). Bernstein and Shapiro<sup>16</sup> also showed that, by measuring the  $\theta$  frequency distributions of glass fibers in a turbulent pipe flow, the fibers aligned in the plane 2-3 were few. Thus we can take simplified steady-state conditions,  $\psi'(\theta = \pi/2) \approx 0$  and  $\bar{\psi}'(\theta = \pi/2) \approx 0$ , and the boundary condition for  $\psi'$  is given by

$$\psi'(\theta = \pi/2, \phi = \sigma, \tau = 0) = 0. \quad (32)$$

Solving Eqs. (29)–(31) with the condition (32), we get

$$\psi' = (1 - \lambda c_{2\theta})^{-3/2} \int_0^\tau h(\tau_0, \sigma) d\tau_0, \quad (33)$$

where

$$h(\tau, \sigma) = (1 - \lambda c_{2\theta})^{3/2} \cdot Q. \quad (34)$$

Knowing  $\dot{\phi}$  is very small and can be neglected for the particles with large aspect ratio as shown in Eq. (18), we can write Eq. (33) as

$$\psi' = (1 - \lambda c_{2\theta})^{-3/2} \int_{\pi/2}^\theta (1 - \lambda c_{2\theta_0})^{3/2} \frac{Q(\theta_0)}{\bar{\theta}(\theta_0)} d\theta_0. \quad (35)$$

The result of  $\psi'$  allows us to get the relationship between  $\dot{\theta}' \psi'$ ,  $\dot{\phi}' \psi'$  in Eq. (25) and  $\partial \bar{\psi}' / \partial \theta$ ,  $\partial \bar{\psi}' / \partial \phi$ . However, it is difficult to integrate Eq. (35) because  $\bar{\psi}'$  included in  $Q$  is unknown and what we want to get. Therefore, we adopt a successive iteration method as follows. First, the ODF  $\bar{\psi}'^*$  in laminar shear flow is taken as the first-order approximation of  $\bar{\psi}'$  and is substituted into Eq. (26) to get  $Q$ . Then  $\dot{\theta}' \psi'$  and  $\dot{\phi}' \psi'$  are calculated after  $\psi'$  is obtained by integrating Eq. (35). The dispersion coefficients can be calculated based on  $\dot{\theta}' \psi'$ ,  $\dot{\phi}' \psi'$  and  $\partial \bar{\psi}' / \partial \theta$ ,  $\partial \bar{\psi}' / \partial \phi$ . Finally, the equation of  $\bar{\psi}'$  with these dispersion coefficients is solved to obtain  $\bar{\psi}'$ . The reason for taking  $\bar{\psi}'^*$  as the first-order approximation of  $\bar{\psi}'$  is that Krushkal and Gallily<sup>11</sup> concluded that for flow with mean velocity gradients, the orientation distribution function is anisotropic if the turbulent intensity is not large enough to randomize the particles, and Bernstein and Shapiro<sup>16</sup> found that at laminar flow, the particles are randomly distributed, while at turbulent flow, the randomizing effect of the turbulence also leads to nearly isotropic orientation.

According to the above description,  $Q$  is given by  $\bar{\psi}'^*$  instead of  $\bar{\psi}'$  based on Eq. (26):

$$Q = -f_1 (1 - \lambda c_{2\theta})^{-3/2} \cdot \xi', \quad (36)$$

where

$$\xi' = \frac{6\lambda s_\theta c_\theta}{(\lambda c_{2\theta} - 1)} \dot{\theta}' + \chi' \quad (37)$$

and

$$\chi' = (\lambda s' - w') : \delta_R \delta_R. \quad (38)$$

Equation (35) can be changed to

$$\psi' = -f_1 (1 - \lambda c_{2\theta})^{-3/2} \xi', \quad (39)$$

where

$$\xi' = \int_{\pi/2}^\theta \frac{\xi'(\theta_0)}{\bar{\theta}(\theta_0)} d\theta_0. \quad (40)$$

## 3. Dispersion coefficient

From the physical view,  $\dot{\theta}' \psi'$  and  $\dot{\phi}' \psi'$  can be related to the gradient of the mean ODF  $\bar{\psi}'$  by a dispersion coefficient, i.e.,

$$J_\theta = -\dot{\theta}' \psi' = D_\theta \frac{\partial \bar{\psi}'}{\partial \theta}, \quad (41)$$

$$J_\phi = -\dot{\phi}' \psi' = D_\phi \frac{\partial \bar{\psi}'}{\partial \phi}, \quad (42)$$

where  $\bar{\psi}'$  is also replaced by  $\bar{\psi}'^*$  as a first-order approximation with the same reason. However,  $D_\phi$  is infinite if  $\bar{\psi}'^*$  is uniform in the  $\phi$  direction. Bernstein and Shapiro's experimental results<sup>16</sup> for  $\phi$  distributions confirm that the ODF is random along the  $\phi$  in the turbulent regime. So we give away the meaningless  $D_\phi$  and turn to the available quantity,  $J_\phi$ .

The coefficients are determined from Eq. (39) for  $\psi'$  and Eq. (21) for  $\bar{\psi}^*$ ,

$$D_\theta = \frac{-\overline{\dot{\theta}'\psi'}}{\overline{\partial\bar{\psi}^*/\partial\theta}} = \frac{f_1(1-\lambda c_{2\theta})^{-3/2}\overline{\dot{\theta}'\zeta'}}{-(3/2)f_1(1-\lambda c_{2\theta})^{-5/2}\cdot 2\lambda s_{2\theta}} = -\frac{(1-\lambda c_{2\theta})}{3\lambda s_{2\theta}} \cdot \overline{\dot{\theta}'\zeta'}, \tag{43}$$

$$J_\phi = -\overline{\dot{\phi}'\psi'} = f_1(1-\lambda c_{2\theta})^{-3/2} \cdot \overline{\dot{\phi}'\zeta'}, \tag{44}$$

where  $\zeta'$  is given by Eq. (40).

The quantities  $\overline{\dot{\theta}'\zeta'}$  and  $\overline{\dot{\phi}'\zeta'}$ , included in Eqs. (43) and (44), can be written in detail. First, we let

$$\begin{aligned} \varepsilon'_1 &= k'_{11}, & \varepsilon'_2 &= k'_{12}, & \varepsilon'_3 &= k'_{13}, \\ \varepsilon'_4 &= k'_{21}, & \varepsilon'_5 &= k'_{22}, & \varepsilon'_6 &= k'_{23}, \\ \varepsilon'_7 &= k'_{31}, & \varepsilon'_8 &= k'_{32}, & \varepsilon'_9 &= k'_{33}. \end{aligned} \tag{45}$$

From Eq. (40) we obtain

$$\zeta' = \sum_{i=1}^9 d_i \varepsilon'_i, \tag{46}$$

where

$$\begin{aligned} d_1 &= 3\lambda(1-\lambda) \cdot t_1(\theta, \phi), & d_2 &= d_3 = 0, \\ d_4 &= 6\lambda c_\phi \cdot t_2(\theta, \phi), & d_5 &= 6\lambda(\lambda+1)c_\phi^2 \cdot t_3(\theta, \phi), \\ d_6 &= 6\lambda(\lambda+1)s_\phi c_\phi \cdot t_3, \\ d_7 &= 6\lambda s_\phi \cdot t_2, & d_8 &= d_6, & d_9 &= 6\lambda(\lambda+1)s_\phi^2 \cdot t_3, \end{aligned} \tag{47}$$

where

$$t_1 = \frac{2}{c_\phi \dot{\gamma}} \int_{\pi/2}^\theta \frac{c_{\theta_0}^2}{(\lambda c_{2\theta_0} - 1)^2} d\theta_0, \tag{48}$$

$$t_2 = \frac{2}{c_\phi \dot{\gamma}} \int_{\pi/2}^\theta \frac{s_{\theta_0} c_{\theta_0}}{(\lambda c_{2\theta_0} - 1)^2} d\theta_0, \tag{49}$$

$$t_3 = \frac{2}{c_\phi \dot{\gamma}} \int_{\pi/2}^\theta \frac{s_{\theta_0}^2}{(\lambda c_{2\theta_0} - 1)^2} d\theta_0. \tag{50}$$

At the same time, the fluctuating angular velocities characterized by Eqs. (27) and (28) can be given by

$$\dot{\theta}' = \sum_{i=1}^9 a_i \varepsilon'_i, \tag{51}$$

where

$$\begin{aligned} a_1 &= -\lambda s_\theta c_\theta, & a_2 &= -\frac{1}{2}(1-\lambda c_{2\theta})c_\phi, \\ a_3 &= -\frac{1}{2}(1-\lambda c_{2\theta})s_\phi, \\ a_4 &= \frac{1}{2}(\lambda c_{2\theta}+1)c_\phi, & a_5 &= \lambda s_\theta c_\theta c_\phi^2, & a_6 &= \lambda s_\theta c_\theta s_\phi c_\phi, \\ a_7 &= \frac{1}{2}(\lambda c_{2\theta}+1)s_\phi, & a_8 &= a_6, & a_9 &= \lambda s_\theta c_\theta s_\phi^2, \end{aligned} \tag{52}$$

and

$$\dot{\phi}' = \sum_{i=1}^9 b_i \varepsilon'_i, \tag{53}$$

where

$$\begin{aligned} b_1 &= 0, & b_2 &= \frac{(1-\lambda)c_\theta s_\phi}{2s_\theta}, & b_3 &= -\frac{(1-\lambda)c_\theta c_\phi}{2s_\theta}, \\ b_4 &= -\frac{(\lambda+1)c_\theta s_\phi}{2s_\theta}, & b_5 &= -\lambda s_\phi c_\phi, & b_6 &= -\frac{1}{2}(1-\lambda c_{2\phi}), \\ b_7 &= \frac{(\lambda+1)c_\theta c_\phi}{2s_\theta}, & b_8 &= \frac{1}{2}(\lambda c_{2\phi}+1), & b_9 &= \lambda s_\phi c_\phi. \end{aligned} \tag{54}$$

We can now give the self-governed equation for the mean ODF:

$$\frac{1}{s_\theta} \frac{\partial(s_\theta \overline{\dot{\theta}'\psi})}{\partial\theta} + \frac{\partial(\overline{\dot{\phi}'\psi})}{\partial\phi} = \frac{1}{s_\theta} \frac{\partial}{\partial\theta} \left( s_\theta D_\theta \frac{\partial\bar{\psi}}{\partial\theta} \right) + \frac{\partial(J_\phi)}{\partial\phi}, \tag{55}$$

where

$$D_\theta = -\frac{(1-\lambda c_{2\theta})}{3\lambda s_{2\theta}} \cdot \sum_{i=1}^9 \sum_{j=1}^9 (a_i d_j \cdot \overline{\varepsilon'_i \varepsilon'_j}), \tag{56}$$

$$J_\phi = f_1(1-\lambda c_{2\theta})^{-3/2} \cdot \sum_{i=1}^9 \sum_{j=1}^9 (b_i d_j \cdot \overline{\varepsilon'_i \varepsilon'_j}). \tag{57}$$

The left side of Eq. (55) is the convection terms due to the mean motion of cylindrical particles, while the right is the dispersion terms due to the random motion. The first dispersion term, described by two-order derivatives, introduces a flux opposite to the gradient of the mean ODF. The dispersion along  $\phi$  is characterized by a flux through  $\phi$  angle. Equation (55) together with Eqs. (56) and (57) provides a bridge to understand the influence of turbulent fluids on the ODF of cylindrical particles suspended in turbulent shear flows.

The above procedures are concerned with the simple shear flows. Actually the present analytic approach can be extended to a more general class of flows. However, for a general flow with nonzero velocity gradient, the principal problem is how to obtain  $\psi'$  by integrating Eq. (35).

### III. ORIENTATION DISTRIBUTION IN PIPE FLOW

In this section, the ODF of cylindrical particles of various aspect ratios suspended in laminar and turbulent pipe

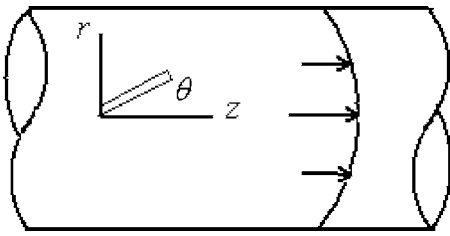


FIG. 2. Pipe and cylindrical particle.

flows, as shown in Fig. 2, is calculated. For turbulent flows, the fluctuating velocity field of fluids is calculated numerically using a kinetic simulation sweeping model (KSSM). The numerical results of the orientation distribution for aspect ratio of 10 are compared with the measured data given by Bernstein and Shapiro<sup>16</sup> in a pipe with diameter of 38 mm.

### A. Orientation distribution in laminar regime

The analytic solution of  $\psi$  in laminar shear flow has been given by Eq. (21), where the coefficient  $f_1$  can be calculated by the normalization condition [Eq. (4)]. For example,  $f_1$  is equal to 0.0883 for the particles with aspect ratio of 10. The results of  $\psi$  in Fig. 3 show that the majority of the cylindrical particles are nearly aligned with the flow direction, and the increase of the particle aspect ratio leads to a more preferred alignment around the flow direction.

In order to compare with the measured results given by Bernstein and Shapiro,<sup>16</sup> an important quantity characterizing the distribution of the frequency of the particle Euler angles is defined:

$$F(\theta_i) = \int_{\theta_i - \frac{\Delta\theta}{2}}^{\theta_i + \frac{\Delta\theta}{2}} \int_0^\pi \psi \sin \theta d\phi d\theta, \quad (58)$$

where  $\theta_i (i=1, 2, \dots, n)$  are the various characteristics of  $\theta$ , and  $\Delta\theta$  is an angle range around  $\theta_i$ . Thus, the  $\theta$  frequency distribution satisfies the following equation:

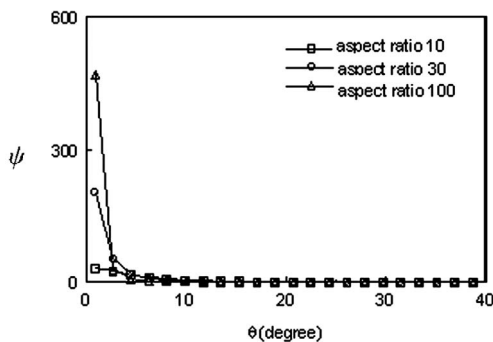
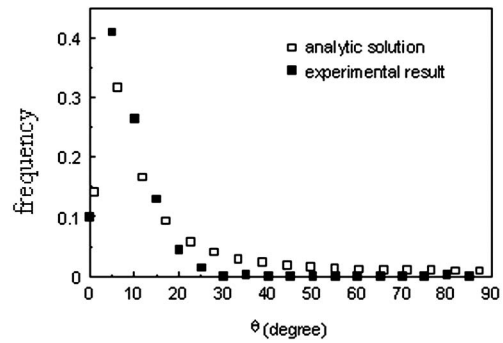
FIG. 3. ODF in terms of angle  $\theta$  for different aspect ratios.

FIG. 4. Analytic and experimental results of frequency distribution for aspect ratio of 10.

$$\sum_{i=1}^n F(\theta_i) = 1. \quad (59)$$

The results of analytic solution and the measured data for aspect ratio of 10 are compared in Fig. 4, where the experimental data are measured at Reynolds number of 1600. According to Jeffery's results, the period of the rotation of nonspherical particle is

$$T = \frac{2\pi}{\dot{\gamma}} \left( a + \frac{1}{a} \right). \quad (60)$$

So the time reaching the steady ODF increases with the decrease of the shear rate  $\dot{\gamma}$ . It is the reason why Bernstein and Shapiro's data<sup>16</sup> of frequency distribution measured in the vicinity of pipe's center are relatively broad at lower Reynolds numbers.

### B. Orientation distribution in turbulent regime

#### 1. A model for turbulent flow field

In order to simulate the motion of particles, the flow field should be known prior. Because of the heavy workload of the computation on turbulence and the fact that the random drive of flow on particles is what we only want to get, a KSSM (Refs. 20 and 21) is employed here. The fluctuating velocity field of fluid can be represented with a Fourier series as follows:

$$\begin{aligned} \frac{\mathbf{u}(\mathbf{x}, t)}{\mathbf{u}_{\text{rms}}(\mathbf{x})} = \sum_{i=1}^N [ & (\mathbf{b}_i \times \mathbf{k}_i) \cos(\mathbf{k}_i \cdot \mathbf{x} - \omega_i t) \\ & + (\mathbf{c}_i \times \mathbf{k}_i) \sin(\mathbf{k}_i \cdot \mathbf{x} - \omega_i t) ], \end{aligned} \quad (61)$$

where  $N$  is a large constant ( $N=100$  in this paper),  $\mathbf{b}_i$  and  $\mathbf{c}_i$  are vectors composed of Gaussian random numbers, frequency  $\omega_i$  is also Gaussian random number whose standard deviation is the root-mean square (rms) of fluctuating velocity  $\mathbf{u}_{\text{rms}}$ , and wave number  $\mathbf{k}_i$  is an isotropic random vector on the surface of unit sphere. Therefore, the dot product of the coefficient of primary function and the wave-number vector is zero  $[(\mathbf{b}_i \times \mathbf{k}_i) \cdot \mathbf{k}_i = 0]$ , which ensures the flow field incompressible.

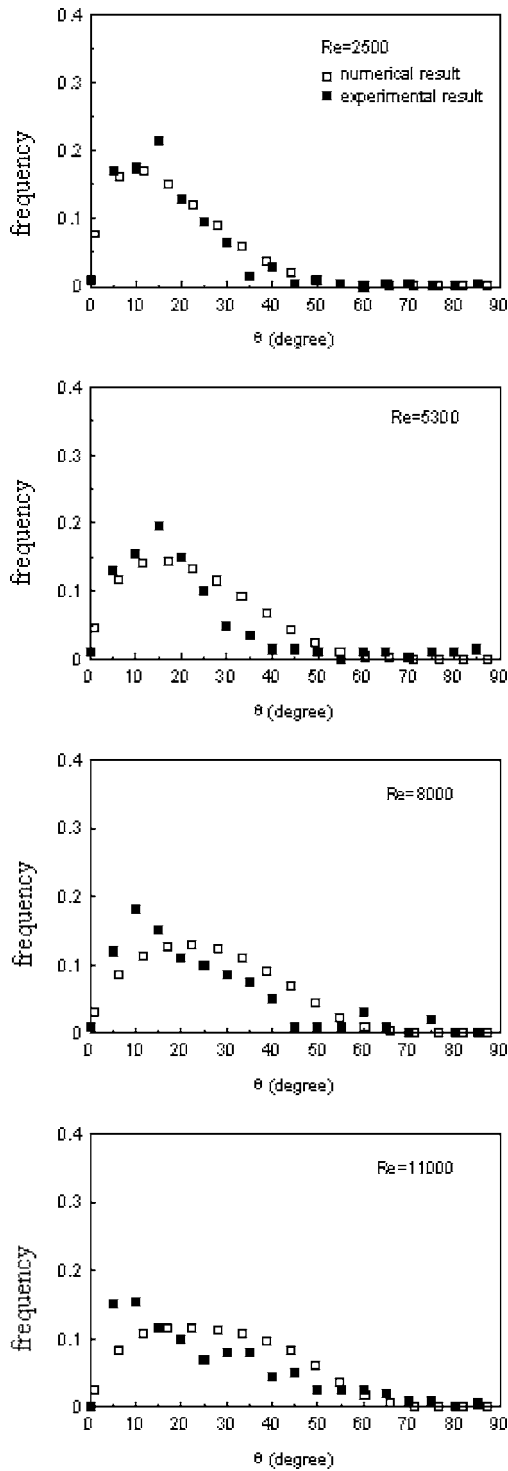


FIG. 5. Numerical and experimental results of  $\theta$  frequency distribution in the vicinity of pipe's center for aspect ratio of 10 at different Reynolds numbers.

According to the definition (45),  $\overline{\varepsilon'_i \varepsilon'_j}$  are the correlations of fluid velocity gradient and can be calculated by using the KSSM model. For a pipe flow, the position coordinate system is defined as

$$1 \rightarrow z, \quad 2 \rightarrow r, \quad 3 \rightarrow \alpha, \tag{62}$$

thus the velocity gradient tensor has the following forms:

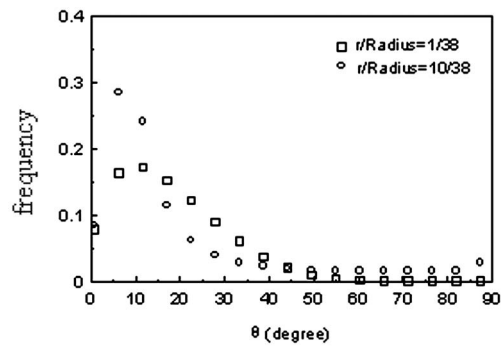


FIG. 6. Numerical results of  $\theta$  frequency distribution for aspect ratio of 10 at Reynolds number 2500 at two radial positions.

$$\begin{aligned} \varepsilon'_1 &= \frac{\partial u'_z}{\partial z}, & \varepsilon'_2 &= \frac{\partial u'_z}{\partial r}, & \varepsilon'_3 &= \frac{\partial u'_z}{r \partial \alpha}, \\ \varepsilon'_4 &= \frac{\partial u'_r}{\partial z}, & \varepsilon'_5 &= \frac{\partial u'_r}{\partial r}, & \varepsilon'_6 &= \frac{\partial u'_r}{r \partial \alpha} - \frac{u'_\alpha}{r}, \\ \varepsilon'_7 &= \frac{\partial u'_\alpha}{\partial z}, & \varepsilon'_8 &= \frac{\partial u'_\alpha}{\partial r}, & \varepsilon'_9 &= \frac{\partial u'_\alpha}{r \partial \alpha} + \frac{u'_r}{r}. \end{aligned} \tag{63}$$

### 2. $\theta$ frequency distribution in pipe flow

The fluid velocity field and the mean ODF are numerically simulated for a pipe flow with the flow Reynolds numbers ranging from 2500 to 11 000. For the symmetry of the pipe flow, the distribution of  $\phi$  is nearly uniform.

Bernstein and Shapiro's data,<sup>16</sup> measured in the vicinity of pipe's center, are compared with our calculated results for the aspect ratio of 10 with the Reynolds number ranging from 2500 to 11 000 as shown in Fig. 5 which shows the influence of Reynolds number on the particle orientation distribution. As the Reynolds number increases the tendency of less alignment becomes more and more visible. It seems that  $\theta$  frequency distributions were uniform at large Reynolds number. Our results compare qualitatively with the experimental data.

The fluid mean shear rate is smaller in the vicinity of pipe's center than that at the positions far from the center axis. The interplay between the mean velocity gradient and the randomizing effect of turbulence is represented in Fig. 6 for the aspect ratio of 10 at the Reynolds number of 2500. It can be seen that more particles are aligned with the  $z$  axis at the position far from the center axis ( $r/\text{radius}=10/38$ ) than that in the vicinity of pipe's center ( $r/\text{radius}=1/38$ ). The wider distribution of  $\theta$  in the vicinity of pipe's center resulted not only from the smaller fluid mean velocity gradient, but also from the larger influence of turbulent dispersion. About the latter we can see the terms  $\varepsilon'_3$ ,  $\varepsilon'_6$ , and  $\varepsilon'_9$ , as shown in Eq. (63). So we can conclude that the turbulent dispersion is dominant for affecting the orientation distribution of particles in the vicinity of the center axis, and the particle rotation due to the mean velocity gradient is more important at the positions far from the center axis.

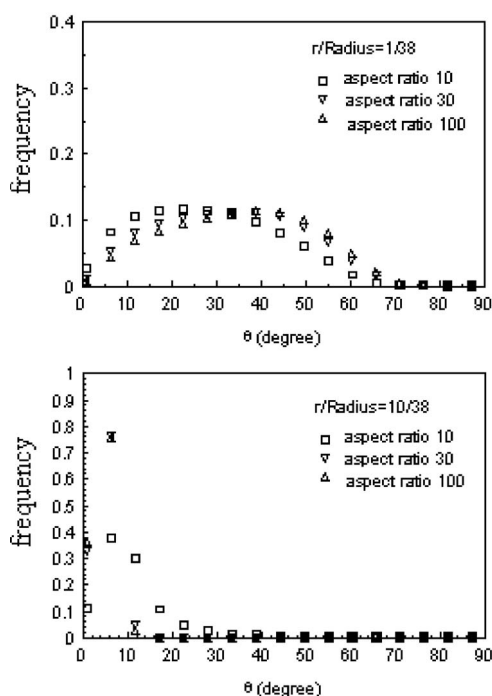


FIG. 7. Numerical results of  $\theta$  frequency distribution at Reynolds number 11000 for different aspect ratios at two radial positions.

In order to examine the effect of the particle aspect ratio on their orientation distribution, we also simulated numerically the  $\theta$  frequency distribution with different aspect ratios. Figure 7 shows the numerical results of the frequency distributions of particles with different aspect ratios at two radial positions. At the position around the center axis, the increase of the aspect ratio leads to a broader distribution of  $\theta$ , which indicates that the particles with larger aspect ratios enhance the turbulent dispersion more obviously. While at the position far from the center axis, the  $\theta$  frequency distribution becomes narrower with the increase of the aspect ratio. This tendency is similar to that in the laminar regime.

#### IV. CONCLUSIONS

A theoretical model for the ODF of cylindrical particles suspended in shear flows is proposed. The fluctuating equation for the ODF of cylindrical particles is theoretically solved using the method of characteristics. The evolution of the mean ODF is described by a modified convection-dispersion equation. The model and modified equation are used to calculate the ODF in a pipe flow numerically. The results, comparing qualitatively with the experimental data, show that the randomizing effect of turbulence leads to a broader orientation distribution of particles, with a tendency of uniform distribution at large Reynolds number. More particles are aligned at the positions far from the center axis than that in the vicinity of the axis. With the increase in the particle aspect ratio, the particles become less aligned with

the flow direction in the vicinity of the axis, while the orientation distributions of particles become narrow at positions far from the axis.

#### ACKNOWLEDGMENT

The author acknowledges the financial support of the National Natural Science Foundation of China (Grant No. 10372090).

- <sup>1</sup>E. S. G. Shaqfeh and G. H. Fredrickson, "The hydrodynamic stress in a suspension of rods," *Phys. Fluids A* **2**, 7 (1990).
- <sup>2</sup>M. D. Rahnama, L. Koch, and E. S. G. Shaqfeh, "The effect of hydrodynamic interactions on the orientation distribution in a fiber suspension subject to simple shear flow," *Phys. Fluids* **7**, 487 (1995).
- <sup>3</sup>L. G. Leal and E. J. Hinch, "The effect of weak Brownian rotation on particles in shear flow," *J. Fluid Mech.* **46**, 685 (1972).
- <sup>4</sup>E. J. Hinch and L. G. Leal, "Time-dependent shear flows of a suspension of particles with weak Brownian rotations," *J. Fluid Mech.* **57**, 753 (1973).
- <sup>5</sup>G. B. Jeffery, "The motion of ellipsoidal particles immersed in a viscous fluid," *Proc. R. Soc. London, Ser. A* **102**, 161 (1922).
- <sup>6</sup>E. Anczurowski and S. G. Mason, "The kinetics of flowing dispersions: III Equilibrium orientations of rods and discs (experimental)," *J. Colloid Interface Sci.* **23**, 533 (1967).
- <sup>7</sup>E. M. Krushkal and I. Gallily, "On the orientation distribution function of non-spherical aerosol particles in a general shear flow-I. the laminar case," *J. Colloid Interface Sci.* **99**, 141 (1984).
- <sup>8</sup>J. A. Olson, "The motion of fibres in turbulent flow, stochastic simulation of isotropic homogeneous turbulence," *Int. J. Multiphase Flow* **27**, 2083 (2001).
- <sup>9</sup>J. A. Olson, I. Frigaard, C. Chan, and J. P. Hamalainen, "Modeling a turbulent fibre suspension flowing in a planar contraction: the one-dimensional headbox," *Int. J. Multiphase Flow* **30**, 51 (2004).
- <sup>10</sup>J. Z. Lin, W. F. Zhang, and Z. S. Yu, "Numerical research on the orientation distribution of fibers immersed in laminar and turbulent pipe flows," *J. Aerosol Sci.* **35**, 63 (2004).
- <sup>11</sup>E. M. Krushkal and I. Gallily, "On the orientation distribution function of non-spherical aerosol particles in a general shear flow-II. The turbulent case," *J. Aerosol Sci.* **19**, 197 (1988).
- <sup>12</sup>J. A. Olson and R. J. Kerekes, "The motion of fibres in turbulent flow," *J. Fluid Mech.* **377**, 47 (1988).
- <sup>13</sup>J. Feng and L. G. Leal, "Pressure-driven channel flows of a model liquid-crystalline polymer," *Phys. Fluids* **11**, 2821 (2000).
- <sup>14</sup>M. K. Lyon, D. W. Mead, R. E. Elliott, and L. G. Leal, "Structure formation in moderately concentrated viscoelastic suspensions in simple shear flow," *J. Rheol.* **45**, 881 (2001).
- <sup>15</sup>G. Sgalari, L. G. Leal, and E. Meiburg, "Texture evolution of sheared liquid crystalline polymers: Numerical predictions of roll-cells instability, director turbulence, and striped texture with a molecular model," *J. Rheol.* **47**, 1417 (2003).
- <sup>16</sup>O. Bernstein and M. Shapiro, "Direct determination of the orientation distribution function of cylindrical particles immersed in laminar and turbulent shear flows," *J. Aerosol Sci.* **25**, 113 (1994).
- <sup>17</sup>G. K. Batchelor, "The stress system in a suspension of force-free particles," *J. Fluid Mech.* **41**, 545 (1970).
- <sup>18</sup>S. M. Dinh and R. C. Armstrong, "A rheological equation of state for semiconcentrated fiber suspensions," *J. Rheol.* **28**, 207 (1984).
- <sup>19</sup>S. G. Advani and C. L. Tucker, "The use of tensors to describe and predict fiber orientation in short fiber composites," *J. Rheol.* **31**, 751 (1987).
- <sup>20</sup>J. C. H. Fung, J. C. R. Hunt, N. A. Malik, and R. J. Perkins, "Kinematic simulation of homogeneous turbulence by unsteady random Fourier modes," *J. Fluid Mech.* **236**, 281 (1992).
- <sup>21</sup>L. P. Wang and D. E. Stock, "Numerical simulation of heavy particle dispersion-scale ratio and flow decay considerations," *ASME J. Fluids Eng.* **116**, 154 (1994).